Addressing the Primary and Subharmonic Resonances of the Swing Equation

ANASTASIA SOFRONIOU, BHAIRAVI PREMNATH
School of Computing and Engineering, University of West London
St. Mary's Road, W5 5RF
UNITED KINGDOM

Abstract: A research investigation is undertaken to gain a more comprehensive understanding of the primary and subharmonic resonances exhibited by the swing equation. The occurrence of the primary resonance is characterised by amplified oscillatory reactions, voltage instability, and the possibility for system failure. The phenomenon of subharmonic resonance arises when the frequency of disturbance is a whole-number fraction of the natural frequency. This results in the occurrence of low-frequency oscillations and the potential for detrimental effects on equipment. The objective of this study is to expand upon the current literature regarding the impacts of primary resonance and enhance comprehension of subharmonic resonance in relation to the stability of a specific power system model. The analytical and numerical tools are utilised to investigate the fundamental principles of this resonant-related problem, aiming to provide an effective control solution. This choice is driven by the model's complex nonlinear dynamical behaviour, which offers valuable insights for further analysis. This analysis includes the Floquet Method, the Method of strained parameters, and the concept of tangent instability in order to provide an extension to existing literature relating to primary and subharmonic resonances, taking into account the dynamic and bifurcation characteristics of the swing equation. This objective will be achieved through the utilisation of both analytical and numerical methods, enabling the identification of specific indicators of chaos that can contribute to the safe operation of real-world scenarios.

Key-Words: nonlinear dynamics, swing equation, resonance, bifurcation, power system

Received: March 15, 2023. Revised: August 14, 2023. Accepted: September 16, 2023. Published: October 13, 2023.

1 Introduction

The swing equation is widely regarded as a fundamental model used to analyse the dynamic characteristics of power systems, with a focus on the oscillatory movement exhibited by synchronous generators. In order to ensure the stability and reliability of electricity infrastructures, it is imperative to have a comprehensive understanding of the resonance events that may arise within this nonlinear system. This equation is subject to two important types of resonance: primary resonance and subharmonic resonance. This manuscript serves as an extension of the preceding research conducted by the authors cited in, [1], [2] whereby their findings are further developed to provide a thorough elucidation of the phenomenon known as subharmonic resonance.

The stability of a dynamical system is significantly influenced by primary and subharmonic resonances. The notion of disturbances, characterised by sudden alterations in the operational variables of a system, is closely interconnected with the notion of stability within a power system. A slight disturbance can yet have a diverse influence on the dynamics of a system, [1]. The dynamic behaviour of the system is examined by manipulating the variables in the equation while holding all other elements constant. The significance of the primary resonance is deemed crucial in the analysis of the swing equation. When fundamental resonance conditions are met, a minor perturbation can lead to a significant response if the frequency of the external force is in close proximity to the linearised natural frequency, [3]. Furthermore, it is worth noting that the steady-state forced response of the nonlinear system may exhibit nonlinear dynamic phenomena, such as saddle-node bifurcations and period doubling bifurcations, [4].

The Floquet approach is a significant tool in the analysis of power system stability, particularly in the context of tiny disruptions, [5], [6]. The mathematical methodology employed in assessing the stability of periodic solutions, such as those seen in the swing equation, involves the examination of the eigenvalues of the linearized equations governing the system. Tangent instability, conversely, refers to a phenomena in which minor disturbances in the operational parameters of a power system can result in prolonged oscilla-

tions or instability, [7]. The strained parameters method is a strategy in control theory that is employed to mitigate tangent instability by modifying system characteristics in order to uphold stability, [8]. Collectively, these notions offer a comprehensive theoretical structure for examining and managing the stability of a mathematical problem, thereby guaranteeing their dependable functioning in the presence of dynamic disturbances.

The phenomenon of primary resonance occurs when the frequency of excitation is in close proximity to the natural frequency of the system. On the contrary, subharmonic resonance occurs when the frequency of stimulation is a multiple of the natural frequency, [9], [10]. A wide range of research have been undertaken to investigate the resonances present in nonlinear power systems, with the aim of comprehending the fundamental principles governing them and developing effective control strategies. Researchers have employed mathematical modelling, computer studies, and experimental validations to examine the impact of primary and subharmonic resonance on the stability of power systems, [1], [2] . In order to mitigate the adverse effects of resonance and enhance the stability of systems, researchers have made significant contributions through the advancement of sophisticated control approaches, including adaptive control, robust control, and damping controllers.

1.1 Brief Literature Review

Ensuring the reliability and efficiency of the functioning of electric circuits depends upon the stability of power systems, hence a deeper understanding is required to prevent chaos happening in the system, [11], [12]. When a power system exhibits stability, it is capable of maintaining its operational state within acceptable limits and preserving its equilibrium despite encountering disturbances. The comprehension of the dynamic behaviour of power systems and other stability concerns is significantly enhanced by the study of the swing equation, [13], [14]. The presence of resonance at both fundamental and subharmonic frequencies is a significant factor that might potentially influence the stability of a system. Transient stability and steady-state stability are the primary classifications of this power system's stability. Transient stability is the term used to describe the ability of a system to regain a stable operational state after experiencing a notable disturbance, such as a fault or an abrupt reduction in load, [15]. The topic of steady-state stability, commonly referred to as small-signal stability, pertains to the system's capacity to maintain stability even when confronted with little disturbances, such as mild fluctuations in power consumption or generation, [16].

The swing equation is a fundamental dynamic equation employed for the purpose of simulating the behaviour of synchronous generators within a power system. This paper elucidates the transient behaviour of synchronous machines, specifically focusing on the speed dynamics and rotor angle stability. The swing equation is based on the premise that the electrical output of a generator is inversely proportional to the angle formed between its rotor and the voltage of the system at its terminal, [17], [18]. Primary resonance occurs when the natural frequency of a power system aligns with the frequency of an externally imposed disturbance. The phenomenon described has the potential to induce oscillations that lack stability leading to instability within the system, [19], [20]. The phenomenon of primary resonance often arises in the context of electromechanical oscillation modes characterised by low frequencies. This phenomenon is commonly observed in the interaction between generators and their respective control systems, [21]. According to the cited source, [22], the occurrence of substantial oscillations in generator rotor angles has the potential to result in cascading failures and subsequent blackouts if not promptly addressed. Subharmonic resonance refers to a phenomena observed in power systems, when the system's response exhibits oscillations at frequencies that are lower than the frequency of the external disturbance delivered to it, [23], [24]. This arises when the natural frequency of a power system decreases to a level below the frequency of a disturbance. Power electronic components, such as voltage source converters or thyristor-controlled reactors, have the potential to induce subharmonic resonance when interacting with the power system, [25]. If left unmitigated, this phenomenon has the potential to lead to persistent oscillations and instability. According to the literature, [26], [27], it is imperative to consider subharmonic resonance while designing and operating power electronic equipment that is connected to the grid.

Understanding the unique attributes and implications for power system stability necessitates a thorough examination and comparison of primary and subharmonic resonance. In the study conducted by the authors cited in, [28], a combination of analytical and experimental methodologies was employed to undertake a comprehensive analysis and comparison of the two resonance events. The study conducted by the researchers

shed insight on the similarities and differences between primary and subharmonic resonance, emphasising the importance of conducting a comprehensive investigation, [29]. The advancement of categorization methodologies has facilitated enhanced discernment and distinction between fundamental and subharmonic resonance phenomena. Previous studies have provided evidence to support the notion that machine learning methods, including neural networks and support vector machines, has the capability to effectively classify different resonance variations. The researchers in the cited studies, [30], [31] introduced a methodology based on neural networks to classify resonance phenomena in real-time, enabling prompt detection and response to significant stability events. The authors in the cited publication not only conducted an analysis on the impact of control strategies on subharmonic resonance, but also underscored the need of accounting for variations in system parameters when assessing the dynamic characteristics of main and subharmonic resonances.

The investigation of power system stability has been the focus of substantial scholarly inquiry, resulting in the development of many methodologies aimed at comprehending the complex dynamics of synchronous machines. Significant attention has been given to the Floquet method, method of strained parameters, and examination of tangent instability within the framework of the swing equation. The Floquet approach, which is based on the principles of linear periodic systems, has demonstrated its efficacy as a valuable technique for evaluating the stability of systems under periodic disturbances, [32]. This method provides valuable information regarding stability boundaries and bifurcation occurrences. In the context of system analysis, the utilisation of strained parameters enables a detailed investigation into the dynamics of the system across different operational scenarios. This approach facilitates a more profound understanding of the swing equation's responsiveness to alterations in its parameters, [33]. Furthermore, the investigation of tangent instability has provided a deeper understanding of the crucial significance of bifurcations in the dynamics of power systems, hence providing significant knowledge regarding the occurrence of chaotic phenomena, [34]. The utilisation of these methodologies collectively contributes to the advancement of comprehensive stability assessment procedures for power systems, hence augmenting their dependability and ability to withstand adverse conditions.

Basins of attraction refer to spatial regions inside the state space wherein the system's trajectories converge towards specific attractors. Numerous investigations have been conducted to analyse the basins of attraction associated with fundamental and subharmonic resonance phenomena in power systems. In these investigations, researchers have applied a range of approaches such as bifurcation analysis, numerical simulations, and Lyapunov exponent calculations to ascertain the borders and properties of the basins of attraction, [35], [36]. These same techniques will also be implemented in the present study.

2 Methodology

2.1 Analytical Work

The swing equation was developed from the Law of Rotation, a key principle used to characterise the motion of revolving bodies. This law is rooted in Newtonian mechanics, a foundational framework in physics. Synchronous generators demonstrate rotating characteristics when they are interconnected with the electrical grid within the framework of power systems. The derivation of the equation governing the dynamic motion of the generator rotor can be achieved by applying Newton's second law of motion to the synchronous generator. This analysis takes into account the mechanical and electrical torques acting on the rotor, as well as the inertia of the rotating mass and the damping effects. This approach has been discussed in previous studies, [1], [2], [13]. The swing equation is a second-order nonlinear differential equation that describes the temporal variation of the angle deviation of a generator's rotor from its synchronous position.

The equation governing the motion of the rotor of the machine under the study is the swing equation, which includes a damping term is as follows, [13]:

$$\frac{2H}{\omega_R}\frac{d^2\theta}{dt^2} + D\frac{d\theta}{dt} = P_m - \frac{V_G V_B}{X_G}\sin(\theta - \theta_B) \quad (1)$$

$$V_{\mathrm{B}} = V_{B0} + V_{\mathrm{B1}}\cos(\Omega t + \phi_v) \quad (2)$$

$$\theta_B = \theta_{B0} + \theta_{B1}\cos(\Omega t + \phi_0) \quad (3)$$

with
$\omega_R = Constant\ angular\ velocity$,
H= Inertia,
D= Damping,
P_m= Mechanical Power,

V_G= Voltage of machine,
X_G = Transient Reactance,
V_B= Voltage of bus,
θ_B = phase of bus,

V_{B1} and θ_{B1} magnitudes assumed to be small.

In order to enhance one's understanding of the phenomenon of subharmonic resonance, it is imperative to undertake a comprehensive mathematical examination of the swing equation. Several mathematical techniques, such as algebraic procedures, Taylor expansion, and substitution, are utilised in order to accomplish this task. The aim of this study is to derive a comprehensive equation suitable for perturbation analysis, focusing specifically on the investigation of subharmonic resonance inside the swing equation. The utilisation of Taylor expansion facilitates the reduction of complexity associated with specific nonlinear variables present in the swing equation, hence enabling easier manipulation and analysis.

Considering the following transformations,

$$\theta - \theta_B = \delta_0 + \eta \tag{4}$$

$$\delta_0 = \theta_0 - \theta_{B0} \tag{5}$$

$$\eta = \Delta\theta - \theta_{B1}\cos(\omega t + \phi_0) \tag{6}$$

After manipulating equation (1), the following is obtained which is used for further analysis with regard to primary and subharmonic resonances, [2]:

$$\frac{d^2\eta}{dt^2} + \frac{\omega_R D}{2H}\frac{d\eta}{dt} + K\eta = \alpha_2\eta^2 + \alpha_3\eta^3 + G_1\eta\cos(\Omega t + \phi_v) + G_2\eta^2\cos(\Omega t + \phi_v) + G_3\eta^3\cos(\Omega t + \phi_v) + Q\cos(\Omega t + \phi_e).$$

Perturbation Analysis for Subharmonic resonance

This method uses multiple scales to determine second order approximate expression for period-two solutions for the case $\Omega \simeq 2\omega_0$, [2].

The proposed solution has the potential to be utilised for the anticipation of the commencement of intricate dynamics and the assessment of stability. Therefore, the accuracy of the solution diminishes with increasing excitation amplitude due to its failure to incorporate the frequency shift caused by the external stimulation. Introducing a small dimensionless parameter ε, which is used as a bookkeeping device, [2].

Let

$$\eta = O(\varepsilon) \quad then \quad \frac{\omega_R D}{2H} = O(\varepsilon)$$

$$G_1 = O(\varepsilon) \quad Q = O(\varepsilon)$$

and

$$V_{B1} = O(\varepsilon)\ and\ \theta_{B1} = 0(\varepsilon)$$

Then the final equation from swing equation derivation above has the following coefficients,

$$G_1 = \varepsilon g_1$$

$$G_2 = \varepsilon g_2$$

$$G_3 = \varepsilon g_3$$

$$Q = \varepsilon q$$

After mathematical operations, equation (7) is formulated as follows,

$$\ddot{\eta} + 2\varepsilon\mu\dot{\eta} + \omega_0^2\eta = \alpha_2\eta^2 + \alpha_3\eta^3 + \varepsilon g_1\eta\cos(\Omega t + \phi_v) + \varepsilon g_2\eta^2\cos(\Omega t + \phi_v) + \varepsilon g_3\eta^3\cos(\Omega t + \phi_v) + \varepsilon q\cos(\Omega t + \phi_e)$$

where $\mu = \frac{\omega_R D}{4H}$.

The solution to this above equation should be in the form of,

$$\eta(t;\varepsilon) = \varepsilon\eta_1(T_0, T_1, T_2) + \varepsilon^2\eta_2(T_0, T_1, T_2) + \varepsilon^3\eta_3(T_0, T_1, T_2) + \ldots\ldots \tag{8}$$

First derivative of this equation will be,

$$\frac{d}{dt} = D_0 + \varepsilon D_1 + \varepsilon^2 D_2 + ... \tag{9}$$

Second derivative of the equation is,

$$\frac{d^2}{dt^2} = D_O^2 + 2\varepsilon D_0 D_1 + \varepsilon^2(2D_0 D_2 + D_1^2) + ... \tag{10}$$

where

$$D_n = \frac{\partial}{\partial T_n}.$$

Also considering the equation where σ is introduced as a detuning parameter:

$$\omega_0^2 \ = \ \frac{1}{4}\Omega^2 \ + \ \varepsilon\sigma \tag{11}$$

and substituting equations (8), (9), (10) and (11) into (7) gives

$$\ddot{\eta} + 2\varepsilon\mu\dot{\eta} + \left(\frac{1}{4}\Omega^2 + \varepsilon\sigma\right)[\varepsilon\eta_1(T_0,T_1,T_2)$$

$$+ \quad \varepsilon^2\eta_2(T_0,T_1,T_2) \quad + \quad \varepsilon^3\eta_3(T_0,T_1,T_2) \quad + \ldots \quad = \quad \alpha_2\left(\varepsilon^2\eta_1^2 + \varepsilon^4\eta_2^2 + \varepsilon^6\eta_3^2 + \ldots\right) \quad + \alpha_3\left(\varepsilon^3\eta_1^3 + \varepsilon^6\eta_2^3 + \varepsilon^9\eta_3^3 + \ldots\right)$$

$$+ \quad \varepsilon g_1\left(\varepsilon\eta_1 + \varepsilon^2\eta_2 + \varepsilon^3\eta_3\right)\cos\left(\Omega t + \phi_v\right) \quad + \varepsilon g_2\left(\varepsilon^2\eta_1^2 + \varepsilon^4\eta_1^2 + \varepsilon^6\eta_3^2\right)\cos\left(\Omega t + \phi_v\right)$$

$$+ \quad \varepsilon g_3\left(\varepsilon^3\eta_1^3 + \varepsilon^6\eta_2^3 + \varepsilon^9\eta_3^3 + \ldots\right) \quad + \varepsilon q\cos\left(\Omega t + \phi_e\right)$$

Equating coefficients of like powers of ε,

$$\varepsilon/: \ \eta_1 D_0^2 + \frac{1}{4}\eta_1\Omega^2 \ = \ qcos(\Omega t + \phi_e) \tag{12}$$

$$\varepsilon^2/: \ \eta_2 D_0^2 + \ \frac{1}{4}\eta_2\Omega^2 + 2D_0D_1\eta_1 + \sigma\eta_1 \ = \ \alpha_2\eta_1^2 + \mathrm{g}_1\eta_1 cos(\Omega T_0 + \ \phi_v) \tag{13}$$

$$\varepsilon^3/: \ D_0^2\eta_3 + 2D_0D_1\eta_2 + (D_1^2 + 2D_0D_2)\eta_1 + \mu D_0\eta_1 + \frac{1}{4}\Omega^2\eta_3 + \sigma\eta_2 = \ 2\alpha_2\eta_1\eta_2 + \alpha_3\eta_1^3 + g_1\eta_2 cos(\Omega T_0 + \phi_v) + \mathrm{g}_2\eta_1^2 cos(\Omega T_0 + \ \phi_v) \tag{14}$$

As also seen in, [2] the solution to equation (12) can be in two forms,

$$(i) \ \eta_1 \ = \ a(T_0,T_1,T_2) \ cos \ [\frac{1}{2}\Omega T_0 \ + \ \beta(T_0,T_1,T_2)] + 2\Lambda cos(\Omega T_0 \ + \phi_e). \tag{15}$$

$$(ii) \ \eta_1 \ = \ A(T_1,T_2)e^{\frac{1}{2}i\Omega T_0} \ + \ \bar{A}(T_1,T_2)e^{\frac{-1}{2}i\Omega T_0} + \ \Lambda e^{i\Omega T_0} \ + \ \bar{\Lambda}e^{-i\Omega T_0}. \tag{16}$$

It is given that

$$N \ = \frac{-2q}{3\Omega^2}e^{i\phi_e} \tag{17a}$$

Comparing coefficients in equations (15) and (16) gives:

$$A \ = \frac{1}{2}ae^{i\beta} \tag{17b}$$

Substituting equation (16) in (13) and rearranging the terms gives the following,

$$D_0^2\eta_2 \ + \ \frac{1}{4}\Omega^2\eta_2 \ = \ e^{\frac{1}{2}i\Omega T_0}[-\sigma A \ + \ 2\alpha_2 N\bar{A} - \Omega i(D_1A \ + \ \mu A) \ + \ \tfrac{1}{2}g_1\bar{A}e^{i\phi_v}] + e^{i\Omega T_0}[-\sigma N + \alpha_2A^2 - 2i\mu\Omega N] + e^{\frac{3}{2}i\Omega T_0}[\tfrac{1}{2}Af_1e^{i\phi v}] + e^{2i\Omega T_0}[\alpha 2N_2 + 12g_1Ne^{i\phi v}] \ + \ [\alpha_2(A\bar{A} \ + \ N\bar{N}) \ + \ 12Ng_1e^{i\phi v}] \ + \ \bar{c}. \tag{18}$$

where $\bar{c}$ is the complex conjugate, as in, [2].

Eliminating the secular terms,

$$-i\Omega D_1A - i\Omega\mu A - \sigma A + \bar{A}\Gamma e^{i\phi_{ee}} \ = \ 0 \tag{19}$$

where

$$\Gamma e^{\phi_{ee}} \ = \ 2\alpha_2N + \ \frac{1}{2} \ g_1e^{i\phi_v} \tag{20}$$

The solution of equation (18) is of the form,

$$\eta_2 \ = \ \frac{-4}{3\Omega^2}[\alpha_2A^2 - (2i\mu\Omega + \sigma)N]e^{iT_0} - \frac{A}{2\Omega^2}\Gamma e^{i(\frac{3}{2}\Omega T_0 + \phi_e e)} + \frac{4}{\Omega^2}[\alpha_2(A\bar{A} + N\bar{N}) + 12g_1Ne^{i\phi v}] - \frac{4}{15\Omega^2}[\alpha_2N^2 + 12\mathrm{g}_1Ne^{i\phi v}]e^{i2\Omega T_0} + \bar{c} \tag{21}$$

Substituting equations (16) and (21) into (14) gives,

$$D_0^2\eta_3 + \frac{1}{4}\Omega^2\eta_3 \ = \ -i\Omega D_2A - D_1^2A \ - 2\mu D_1A - \frac{-8\alpha_2}{3\Omega^2}\left[-(2i\mu\Omega + \sigma)\,N\bar{A} + \alpha_2A^2\bar{A}\right] - \frac{\alpha_2A\bar{\Lambda}}{\Omega^2}\Gamma e^{i\phi_e e} +$$

$$\frac{8\alpha_2}{\Omega^2}[2\alpha_2 A^2\bar{A}+2\alpha_2 AN\bar{N}+\frac{1}{2}g_1A(\bar{N}e^{i\phi_v}+Ne^{-i\phi_v})]+$$

$$6\alpha_3 AN\bar{N} + 3\alpha_3 A^2\bar{A} - \frac{A_1 g_1\Gamma}{4\Omega^2}e^{i(\phi_e e-\phi_v)} + g_2A(\bar{N}e^{i\phi_v}+Ne^{-i\phi_v})+NST+\bar{c} \quad (22)$$

where NST is the not significant terms and $\bar{c}$ is the complex conjugate.

$$\mathrm{D}_1A = -(\mu+\frac{i\sigma}{\Omega})\,\bar{A}+\frac{i}{\Omega}\bar{A}\Gamma e^{i\phi_{ee}} \quad (23)$$

$$\mathrm{D}_1^2A = [\mu^2 - \frac{2i\mu\sigma}{\Omega} + \frac{\Gamma^2-\sigma^2}{\Omega^2}]A + \frac{2i\mu}{\Omega}\bar{A}\Gamma e^{i\phi_{ee}} \quad (24)$$

Eliminating the secular terms in equation (22) and then substituting equations (19) and (24);

$$\text{-i}\Omega D_2A + [\mu^2 - \frac{\Gamma^2-\sigma^2}{\Omega^2} - \frac{\alpha_2\bar{N}\Gamma}{\Omega^2}\,e^{i\phi_{ee}} + (6\alpha_3+\frac{16\alpha_2^2}{\Omega^2})N\bar{N} + (\bar{N}e^{i\phi_v}+Ne^{-i\phi_v})\,(\frac{4\alpha_2 f_1}{\Omega^2}+f_2) - \frac{\Gamma f_1}{4\Omega^2}e^{i(\phi_{ee}-\phi_v)}]A + (3\alpha_3+\frac{40(\alpha_2)^2}{32})A^2\bar{A} + \frac{8_2}{3\Omega^2}(2i\mu\Omega+\sigma)NA = 0 \quad (25)$$

Using method of reconstitution, the derivative of A with respect to t is found and substituting equation (19) and (25) into equation (9) and equating ε= 1, gives the following,

$$\mathrm{i}\Omega(\dot{A}+\mu_eA) + \sigma_eA - 4\alpha_eA^2\bar{A} - \hat{\Gamma}e^{i\hat{\phi}_e} = 0 \quad (26)$$

where $\mu_e = \mu - \frac{2\alpha_2 q\Gamma}{3\Omega^5}\,sin\,(\phi_{ee}-\phi_e) + \frac{\Gamma g_1}{4\Omega^3}\,sin\,(\phi_{ee}-\phi_v)$. (27)

Also $\sigma_e = \sigma - \mu^2 + \frac{\Gamma^2-\sigma^2}{\Omega^2} - (\frac{2q}{3\Omega^2})^2\,(6\alpha_3 + \frac{16\alpha_2^2}{\Omega^2}) + \frac{4q}{3\Omega^2}(g_2+\frac{4\alpha_2 g_1}{\Omega^2})cos(\phi_v-\phi_e) - \frac{2q\Gamma\alpha_2}{3\Omega^4}\,cos(\phi_{ee}-\phi_e) + \frac{\Gamma g_1}{4\Omega^2}\,cos\,(\phi_{ee}-\phi_v)$ (28)

where $\alpha_e = \frac{10\alpha_2^2}{3\Omega^2} + \frac{3}{4}\,\alpha_3$ (29)

and

$$\hat{\Gamma}e^{i\hat{\phi}_e} = \Gamma e^{i\phi_{ee}} - \frac{16\alpha_2 q}{9\Omega^4}\,(2i\mu\Omega+\sigma)\,e^{i\phi_e}. \quad (30)$$

Separating the real and imaginary parts gives the equations below,

$$\Omega(\dot{a}+\mu_ea) - a\hat{\Gamma}sin\gamma = 0 \quad (31)$$

$$\text{-}\Omega a\dot{\beta} + \sigma_ea - \alpha_ea^3 - a\hat{\Gamma}cos\gamma = 0 \quad (32)$$

where $\gamma = \hat{\phi}_e - 2\beta$. (33)

Therefore

$$\eta = acos[\frac{1}{2}cos(\Omega t+\hat{\phi}_e-\beta)]-\frac{4q}{3\Omega^2}cos(\Omega t+\phi_e)+$$

$$\frac{32\mu q^2}{9\Omega^3}sin(\Omega t+\phi_e)-\frac{16\sigma q}{9\Omega^4}cos(\Omega t+\phi_e)-$$

$$\frac{2a^2\alpha_2}{3\Omega^2}cos(\Omega t+\hat{\phi}_e-\gamma)-\frac{32\alpha_2 q}{135\Omega^6}cos[2(\Omega t+\phi_e)]-$$

$$\frac{ag_1}{4\Omega^2}cos[\frac{3}{2}\Omega t+\phi_v+\frac{1}{2}(\phi_e-\gamma)]+\frac{2\alpha_2}{\Omega^2}(a^2+\frac{16q^2}{9\Omega^4})-$$

$$\frac{8g_1q}{3\Omega^4}cos(\phi_v-\phi_e)+\frac{2\alpha_2 aq}{3\Omega^4}cos[\frac{3}{2}\Omega t+\phi_e+\frac{1}{2}(\hat{\phi}_e-\gamma)]+$$

$$\frac{8g_1q}{45\Omega^4}cos(2\Omega t+\phi_e+\phi_v)+.... \quad (34)$$

$$\Delta\theta = \theta_{B1}\,cos(\Omega t+\phi_\theta)+acos[\frac{1}{2}(\Omega t+\hat{\phi}_e-\beta)]-$$

$$\frac{4q}{3\Omega^2}cos(\Omega t+\phi_e)+\frac{32\mu q}{9\Omega^3}sin(\Omega t+\phi_e)-$$

$$\frac{16\sigma q}{9\Omega^4}cos(\Omega t+\phi_e)-\frac{2a^2\alpha_2}{3\Omega^2}cos(\Omega t+\hat{\phi}_e-\gamma)+$$

$$\frac{2\alpha_2 aq}{3\Omega^4}cos[\frac{3}{2}\Omega t+\hat{\phi}_e+\frac{1}{2}(\phi_e-\gamma)]-$$

$$\frac{ag_1}{4\Omega^2}cos[\frac{3}{2}\Omega t+\phi_v+\frac{1}{2}(\phi_e-\gamma)]+\frac{2\alpha_2}{\Omega^2}(a^2+\frac{16q^2}{9\Omega^4})+$$

$$\frac{8g_1q}{3\Omega^4}cos(\phi_v-\phi_e)+\frac{32\alpha_2q^2}{135\Omega^6}cos[2(\Omega t+\phi_e)]+$$

$$\frac{8g_1q}{45\Omega^4}cos(2\Omega t+\phi_e+\phi_v)+.... \quad (35)$$

Letting $\dot{a}=\dot{\beta}=0$ in equations (31), (32) and (33),

$$\Omega\mu_ea - \hat{\Gamma}a\,sin\gamma = 0 \quad (36)$$

$$\sigma_ea - \alpha_ea^3 + \hat{\Gamma}a\,cos\gamma = 0 \quad (37)$$

When a=0,

$$\Delta\theta = \theta_{B1}\, cos(\Omega t + \phi_\theta) - \frac{4q}{3\Omega^2} cos(\Omega t + \phi_e) +$$

$$\frac{32\mu q}{9\Omega^3} sin(\Omega t + \phi_e) - \frac{16\sigma q}{9\Omega^4} cos(\Omega t + \phi_e) + \frac{32\alpha_2 q^2}{9\Omega^6} -$$

$$\frac{8g_1 q}{3\Omega^4} cos(\phi_v - \phi_e) + \frac{32\alpha_2 q^2}{135\Omega^6} cos[2(\Omega t + \phi_e)] +$$

$$\frac{8g_1 q}{45\Omega^4} cos(2\Omega t + \phi_e + \phi_v) \quad (38)$$

which is similarly echoed in, [2], [6].

When a $\neq 0$, eliminating γ to obtain the frequency response equation,

$$\mathrm{a}^2 = \frac{1}{\alpha_e}[\sigma_e \pm \sqrt{(\hat{\Gamma}^2 - \Omega^2\mu_e^2)}] \quad (39)$$

The frequency response plot is obtained with regard to equation (39) which shows the numerical simulation and perturbation solution.

To facilitate the comparison between analytical findings and numerical simulations in the context of subharmonic resonance, Figure 1 is provided. This figure showcases phase portraits and time histories at a frequency of $\Omega = 26.01$ rad/sec.

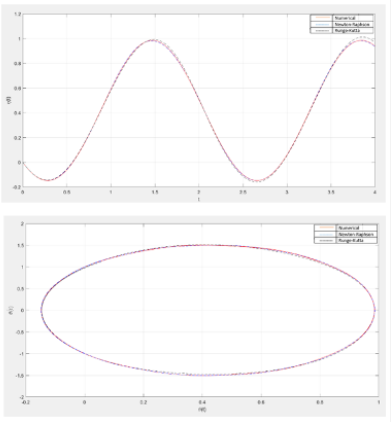

Fig. 1: Perturbed solution employing Runge-Kutta and Newton Raphson algorithms in comparison to numerical simulations for the case of subahrmonic resonance in the phase plane and time history for $\Omega = 26.01$ rad/sec.

The perturbation analysis was simulated and compared to its numerical counterpart using the Runge-Kutta and Newton Raphson methods. The computed numerical errors of the Newton Raphson technique and the Runge-Kutta method, when compared to the actual simulation error, were found to be 0.0995 and 0.0419, respectively. These results indicate that the Newton Raphson method exhibits a better fit, as evidenced by its lower error value.

Floquet Method

Let $u(t)$ be a small disturbance (arbitrary), then,

$$\hat{\eta}(t) = \eta(t) + u(t) \quad (40)$$

The stability of $\eta(t)$ depends on the growth/decay of $u(t)$.

Substituting equation (26) into equation (I) and eliminating any nonlinear terms with $\zeta(t)$ will give

$$\frac{d^2u}{dt^2} + \frac{\omega_R D}{2H}\frac{du}{dt} + u(K - 2\alpha_2\eta - 3\alpha_3\eta^2) = 0 \quad (41)$$

Behaviour of $u(t)$ is obtained from the Floquet theory. If $u_1(t)$, $u_2(t)$ are solutions to equation (41) then $u_1(t+T)$, $u_2(t+T)$ are also solutions to the equation.

Therefore, they are represented as linear combinations as shown below,

$$\mathrm{u}_1(t+T) = a_{11}u_1(t) + a_{12}u_2(t)$$
$$\mathrm{u}_2(t+T) = a_{21}u_1(t) + a_{22}u_2(t)$$

Then two linearly independent solutions are calculated for the initial conditions stated below,

$$u_1(0) = 1$$

$$u_2(0) = 0$$

$$\dot{u}_1(0) = 0$$

$$\dot{u}_2(0) = 1$$

Then the monodromy matrix is obtained,

$$\mathrm{A} = \begin{bmatrix} u_1(T) & \dot{u}_1(T) \\ u_2(T) & \dot{u}_2(T) \end{bmatrix}$$

The eigenvalues are also called the Floquet multipliers. Behaviour of $u(t)$ and the stability of $\eta(t)$ depends on the eigen values. If both multipliers lie inside the unit circle, then it is stable. Analytical solution predicts saddle-node bifurcation accurately.

Method of Strained Parameters

Considering equation (8) and substituting in equation (41) leads to,

$$\ddot{u} + \frac{\omega_R D}{2H}\,\dot{u} + u\,(\,K - 2\alpha_2[\varepsilon a\,cos\,(\Omega t + \beta + \varphi_e) +$$

$$\frac{\varepsilon^2 a^2 \alpha_2}{6\Omega^2}\,[3 - \,cos\,(2\Omega t\, + 2\beta\, +\, 2\varphi_e)]] -$$

$3\alpha_3[[\varepsilon a cos\,(\Omega t + \beta + \varphi_e) + \frac{\varepsilon a 2\alpha_2}{6\Omega^2}[3 - cos(2\Omega t + 2\beta + 2\varphi_e)]]^2) = 0$

Expanding the brackets,

$$\ddot{u} + \frac{\omega_R D}{2H}\,\dot{u} + uK - 2u\alpha_2\varepsilon a\,cos\,(\Omega t + \beta + \varphi_e) +$$

$$\frac{\varepsilon^2 a^2 u\alpha_2^2}{\Omega^2}\; -\; \frac{\varepsilon^2 a^2 u\alpha_2^2}{3\Omega^2} cos\,(2\Omega t\, + 2\beta\, +\, 2\varphi_e) -$$

$3\alpha_3 u\varepsilon^2 a^2 cos^2(\Omega t + \beta + \varphi_e) - \frac{3\alpha_3 u a^3 \varepsilon^2 \alpha_2}{\Omega^2}\; cos\;(\Omega t + \beta + \varphi_e) + \frac{\alpha_3 u\varepsilon^2 a^3 \alpha_2}{\Omega^2}\; cos\;(\Omega t\, +\, \beta\, +\, \varphi_e)\; cos(2\Omega t\, +\, 2\beta\, +\, 2\varphi_e) - \frac{\alpha_3 u\varepsilon^2 a^4 \alpha_2^2}{12\Omega^4}\;(\;(9 + cos(2\Omega t\, +\, 2\beta\, +\, 2\varphi_e) - 6\;cos(2\Omega t\, +\, 2\beta\, +\, 2\varphi_e)\;)\; =\; 0$

From the formulated equation (7),

$$\frac{\omega_R D}{2H}\; =\; 2\varepsilon^2\mu$$

Also considering,

$$\Phi\; = \Omega t\; +\; \beta\; +\; \varphi_e$$

Then the equation will become,

$$\ddot{u}\; +\; 2\varepsilon^2\mu\dot{u}\; +\; uK\; - 2u\alpha_2\varepsilon a\;cos\Phi\; -$$

$$\frac{\alpha_2^2 u\varepsilon^2 a^2}{\Omega^2}\;\frac{\alpha_2 u\varepsilon^2\alpha_2 a^2}{3\Omega^2}\;cos2\Phi\; -$$

$3\alpha_3 u\varepsilon^2 a^2 cos^2\Phi\; -\; \frac{3\alpha_3 u a^3\varepsilon^2\alpha_2}{\Omega^2}\;\; cos\Phi\; +\; \frac{\alpha_3 u\varepsilon^2\alpha_2 a^3}{\Omega^2} cos\Phi\; cos2\Phi\; -\; \frac{3\alpha_3 u\varepsilon^2 a^4\alpha_2^2}{4\Omega^4}\; -$
$\cos^2 2\Phi\;\frac{\alpha_3 u\varepsilon^2\; a^4\alpha_2^2}{12\Omega^4}\; +\; \frac{\alpha_3 u\varepsilon^2 a^4\alpha_2^2}{2\Omega^4}\; =\; 0$

(Cancelling out ε^2 terms)

$$\ddot{u} + 2\mu\dot{u} + uK - 2u\alpha_2\; a\;cos\Phi + \frac{\alpha_2^2 ua^2}{\Omega^2} + \frac{\alpha_2^2 ua^2}{3\Omega^2}\; cos2\Phi$$

$$-\;3\alpha_3 ua^2(\frac{cos\;2\Phi}{2}\; +\; \frac{1}{2}\;)\; -\; \frac{3\alpha_3 ua^3\alpha_2}{\Omega^2}\; cos\;\Phi\; +\; \frac{\alpha_3 ua^3\alpha_2}{\Omega^2}\;\; cos\;\;\Phi\;\; cos\;\;2\Phi\;\; -\;\; \frac{3\alpha_3 ua^4\alpha_2^2}{4\Omega^4}\;\; -\; \frac{cos^2\;2\Phi\;\alpha_3 ua^4\alpha_2^2}{12\Omega^4}\; +\; \frac{\alpha_3 ua^4\alpha_2^2}{2\Omega^2}\; cos\;2\Phi\; =\; 0$$

Simplifying further, the equation below is obtained,

$$\ddot{u} + 2\mu\dot{u} + uK^*\; =\; \chi u\;cos\;\Phi + \Lambda u\;cos\;2\Phi \qquad (42)$$

Where: $\mathrm{K}^*\; = K + \left(\frac{3\alpha_3}{2} - \frac{\alpha_2^2}{3\Omega^2}\right) a^2 - \frac{19\alpha_2^2\;\alpha_e a^4}{24\Omega^4}$

$\chi\; =\; 2\alpha_2 a\; +\; \frac{5\alpha_2\alpha_3 a}{2\Omega^2}$

$\Lambda\; =\; (\frac{3\alpha_3}{2}\; -\; \frac{\alpha_2^2}{3\Omega^2})\; a^2\; -\; \frac{\alpha_2^2\alpha_3 a^4}{2\Omega^4}$

$\Phi\; = \Omega t\; +\; \beta\; +\; \varphi_e \qquad (43)$

Introducing ε which is a small dimensionless parameter as bookkeeping device. Then order damping and parametric term at $0(\varepsilon)$, hence the equation (42) becomes,

$$\ddot{u} + 2\mu\varepsilon\dot{u} + uK^*\; =\; \varepsilon\chi u\;cos\;\Phi + \varepsilon\Lambda u\;cos\;2\Phi \qquad (44)$$

in accordance to, [2], [13].

Uniform expansion of solutions shown below are considered,

$\mathrm{u(t;\varepsilon)}\;\; =\;\; \varepsilon u_1(t)\;\; +\;\; \varepsilon^2 u_2(t)\;\; +\;\; ....$ (45)

$\mathrm{K}^*\;\; =\;\; \frac{1}{4}\Omega^2\;\; +\;\; \varepsilon\;\; \delta_1\;\; +\;\; \varepsilon^2\delta_2\;\; +\;\; ....$ (46)

This determines δ_1, δ_2 and results in periodic expansion, while K^* defines transition curves separating stability from instability giving the curve for period-doubling bifurcation.

Substituting equations (31) and (32) into (30),

$$\ddot{u} + 2\varepsilon\mu\dot{u} + (\frac{1}{4}\Omega^2 + \varepsilon\delta_1 + \varepsilon^2\delta_2 + ...)u\; =\; \varepsilon\chi\;(\varepsilon u_1(t)$$

$$+\;\varepsilon^2 u_2(t)\;\; +\;\; ....)\;\; +\;\; \varepsilon\Lambda\;\; (\varepsilon u_1(t)\;\; +$$
$\varepsilon^2 u_2(t)\;\; +\;\; .....)\; cos\;\; 2\Phi$

Comparing the coefficients of equal powers of ε in the above equation,

Consider $\varepsilon^0\;/:\;\; \ddot{u}_0\;\; +\;\; \frac{1}{4}\;\Omega^2\;\; u_0 =\;\; 0 \qquad (47)$

$\varepsilon^1/:\;\; \ddot{u}_1\;\; +\;\; \frac{1}{4}\;\Omega^2\;\; u_1 =\;\; -2\mu\dot{u}_0\;\; -\;\; \delta_1 u_0\;\; +$ $\chi u_0\;cos\Phi\;\; +\;\; \Lambda\;\; u_0 cos\;\; 2\Phi \qquad (48)$

$\varepsilon^2/:\ddot{u}_2\;\; +\;\; \frac{1}{4}\;\Omega^2\;\; u_2 =\;\; -2\mu\dot{u}_1\;\; -\;\; \delta_1 u_1\;\; -$ $\delta_2 u_2 +\;\; \chi u_1\;\; cos\Phi\;\; +\;\; \Lambda\;\; u_1 cos\;\; 2\Phi \qquad (49)$

Given $\mathrm{u}_0\;\; =\;\; a\cos\;\frac{1}{2}\;\Phi + b\;\sin\;\frac{1}{2}\;\Phi \qquad (50)$

Substituting equation (50) into equation (48)

$$\ddot{u_1} + \frac{1}{4}\,\Omega^2\,u_1 \;=\; -2\mu\dot{u_0} - \delta_1\,(a\,cos\,\frac{1}{2}\,\Phi + b\,cos\,\frac{1}{2}\,\Phi\,)$$

$$+\,\chi cos\;\Phi\;(a\;cos\;\tfrac{1}{2}\;\Phi\;+\;b\;sin\;\tfrac{1}{2}\;\Phi\;)\;+$$

$$\Lambda\;cos\;2\Phi\;(a\cos\tfrac{1}{2}\;\Phi\;+\;b\sin\;\tfrac{1}{2}\Phi)$$

Replacing with,

$$\dot{u_0} \;=\; \frac{-a}{2}\;sin\;\frac{1}{2}\;\Phi\;+\;\frac{b}{2}\;cos\;\frac{1}{2}\;\Phi$$

gives,

$$\ddot{u_1} + \frac{1}{4}\,\Omega^2\,u_1 \;=\; \mu a\Omega\;sin\;\frac{1}{2}\;\Phi\;-\;\mu b\;\Omega\;cos\;\frac{1}{2}\Phi$$

$$-\,\delta_1 a\;cos\tfrac{1}{2}\;\Phi\;-\;\delta_1 a\;sin\tfrac{1}{2}\;\Phi\;+\;a\chi\;cos\Phi\;cos\;\tfrac{1}{2}\;\Phi$$

$$+\;\;b\chi\;cos\Phi\;\sin\;\tfrac{1}{2}\;\Phi\;\;+a\Lambda\;cos\;2\Phi\;cos\;\tfrac{1}{2}\;\Phi\;+$$

$$b\Lambda\;cos\;2\Phi\;sin\tfrac{1}{2}\;\Phi$$

Employing trigonometric identities,

$$\mathrm{a}\chi cos\Phi cos\tfrac{1}{2}\Phi = \tfrac{a\chi}{2}\left(cos\tfrac{3}{2}\Phi + cos\tfrac{1}{2}\Phi\right)$$

$$\mathrm{b}\chi\;cos\Phi\;sin\;\tfrac{1}{2}\;\Phi\;=\;\tfrac{b\chi}{2}\left(sin\tfrac{3}{2}\Phi\;-\;\;sin\tfrac{1}{2}\Phi\right)$$

$$\mathrm{a}\Lambda\;cos\;2\Phi\;cos\;\tfrac{1}{2}\;\Phi\;\;=\;\tfrac{a\Lambda}{2}\left(cos\tfrac{5}{2}\Phi + cos\tfrac{3}{2}\Phi\right)$$

$$\mathrm{b}\Lambda\;cos\;2\Phi\;sin\;\tfrac{1}{2}\;\Phi\;\;=\;\tfrac{b\Lambda}{2}\left(sin\tfrac{5}{2}\Phi\;-\;sin\tfrac{3}{2}\Phi\right)$$

Substituting the above into the equation and rearranging,

$$\ddot{u_1} + \frac{1}{4}\,\Omega^2\,u_1 \;=\; cos\;\frac{1}{2}\;\Phi\;[(\frac{1}{2}\;\chi\;-\;\delta_1)\;a\;-\;\mu b\Omega]+$$

$$sin\frac{1}{2}\Phi[\mu a\Omega - (12\chi + \delta_1)b]+$$

$$\frac{a}{2}(\chi+\Lambda)cos\frac{3}{2}\Phi + \frac{b}{2}(\Phi-\Lambda)sin\frac{3}{2}\Phi + \frac{a\Lambda}{2}cos\frac{5}{2}\Phi -$$

$$\frac{b\Lambda}{2}sin\frac{5}{2}\Phi \qquad (51)$$

For eliminating secular terms in equation (51), consider

$$(\frac{1}{2}\;\chi\;-\;\delta_1)\;a\;-\;\mu b\Omega\;=\;0 \qquad (52)$$

$$\mu a\Omega\;-\;(\frac{1}{2}\;\chi\;+\;\delta_1)b\;=\;0 \qquad (53)$$

It is also given that for non-trivial solution to exist, the following should be satisfied,

$$\delta_1^2\;=\;\tfrac{1}{4}\;\chi^2\;-\;\mu^2\;\Omega^2 \qquad (54)$$

Using equations (52) and (53), equation (51) becomes

$$\mathrm{u}_1\;\;=\;\;D\;\;cos\;\;\tfrac{1}{2}\;\;\Phi\;\;+\;\;E\;\;sin\;\;\tfrac{1}{2}\;\;\Phi\;\;-\;\;\tfrac{(X\;+\;\Lambda)\;a}{4\Omega^2}\;cos\;\tfrac{3}{2}\;\Phi\;-\;\tfrac{(x\;-\;\Lambda)\;b}{4\Omega^2}\;sin\;\tfrac{3}{2}\;\Phi\;+\ldots. \quad (55)$$

D and E constants.

Substituting equations (51) and (55) into equation (50) the following equations are obtained,

$$(\frac{1}{2}\;\chi - \delta_1)\;D - \mu\Omega\;E\;=\;[\delta_2 + \frac{(X\;+\;\Lambda)\;\Lambda}{8\Omega^2}]a \qquad (56)$$

$$\mu\Omega D - \frac{1}{2}\;(\chi + \delta_1)\;E\;=\;[\;\delta_2 + \frac{(X\;-\;\Lambda)\;\Lambda}{8\Omega^2}]b \qquad (57)$$

Given that equations (56) and (57) have non-trivial solution, the inhomogeneous equations have solution if and only if consistency (solvability) condition is satisfied,

$$\delta_2\;\;=\;\;-\;\tfrac{\chi^2\;+\;4\Lambda\delta_1\;+\;\Lambda^2}{8\Omega^2} \qquad (58)$$

Then equation (32) becomes transition curves determining period doubling as shown below,

$$\mathrm{K}^*\;\;=\;\;\tfrac{1}{4}\;\;\Omega^2\;\;\pm\;\;\varepsilon\;(\tfrac{1}{4}\;\chi^2\;-\;\mu^2\;\Omega^2\;)^{1/2}\;\;-$$

$$\varepsilon^2\;\;(\;\tfrac{\chi^2\;+\;4\Lambda\delta_1\;+\;\Lambda^2}{8\Omega^2}\;)^{1/2}\;\;+\;\;\ldots. \quad (59)$$

Tangent Instability

Initially the points corresponding to vertical tangents are in the frequency-response curves given by the equation below, [1],

$$\mu^2\;\;+\;\;(\frac{\sigma}{2\Omega}\;\;+\;\;\frac{\alpha_e a^2}{\Omega})^2\;\;=\;\;\frac{g^2}{4\Omega^2 a^2}$$

Rearranging the above equation,

$$4\mu^2\Omega^2 + (\sigma + 2\alpha_e a^2)^2 = (\tfrac{g}{a})^2 \qquad (60)$$

Also assume: $s = \mathrm{a}^2$

$x = \Omega^2$

$\sigma = \omega_0^2 - \Omega^2$

Then equation (46) is written as: $4\mu^2 xs + s(\omega_0^2 - x - 2\alpha_e s)^2 = g^2$ (61)

Taking the first derivative of equation (61):

$$4\mu^2 x\frac{ds}{dx} + (\omega_0^2 - x - 2\alpha_e s)^2\frac{ds}{dx} - 4\alpha_e s\left(\omega_0^2 - x - 2\alpha_e s\right)\frac{ds}{dx}$$

$$+4\mu^2 s - 2s\left(\omega_0^2 - x - 2\alpha_e s\right) = 0 \qquad (62)$$

Equating the coefficient term of $\frac{ds}{dx} = 0$;

$$4\mu^2 x + (\omega_0^2 - x - 2\alpha_e s)^2 - 4s\alpha_e \left(\omega_0^2 - x - 2\alpha_e s\right) = 0 \quad (63)$$

Substituting equation (61) into (63)
$g^2 = 4s\alpha_e (\omega_0^2 - x - 2\alpha_e s)$ (64)
Let z= $(\omega_0^2 - x - 2\alpha_e s)$ (65)
This equation then can be formulated: $2(z + x - \omega_0^2) = 4\alpha_e s$

Substituting equation (65) into (63)
$4\mu^2 x + z^2 + 4s\alpha_e z = 0$
$4\mu^2 x + z^2 + z\,(2\,(z + x - \omega_0^2)) = 0$

Expanding the brackets and rearranging: $3z^2 + 2z\,(x - \omega_0^2) + 4\mu^2 x = 0$ (66)

In order to calculate the tangent instability using MATLAB, the variable z is determined by solving equation (66) with specific values assigned to the parameter Ω. Subsequently, by solving equation (65) for the variable s and substituting the obtained value into equation (64), the variable g can be determined.

Basins of Attractions
(i) Primary Resonance

The phenomenon of resonance is of utmost importance in understanding the stability characteristics of a nonlinear system. Therefore, it is imperative to conduct a thorough examination of the basins of attraction associated with the primary resonance in order to acquire a thorough understanding of the system. The concept of basins of attraction is utilised in order to delineate the stable and unstable regions within a system, facilitating the analysis of modifications made to said system, [37]. The plots illustrate the alterations in the basins of attraction as variables are modified. When drawing inferences from these graphs, it is imperative to take into account the boundary conditions as well, [38].

Studies of the basins of attraction of primary resonance have revealed significant findings regarding the stability characteristics of power systems. The impact of parameter fluctuations, including system damping, excitation levels, and control gains, on the configuration and amplitude of the basins of attraction linked to primary resonance has been investigated, [39], [40]. Furthermore, scholarly investigations have mostly focused on the identification of crucial borders that demarcate stable and unstable regions within the state space, [41], [42].

(ii) Subharmonic Resonance

This study examines the subharmonic resonance phenomenon and its implications for identifying stable zones within the system. The basins of attraction associated with subharmonic resonance illustrate the areas of stability and instability in a dynamical system when the excitation frequency is nearly twice the natural frequency, [43]. This analysis aims to identify the points of chaos and instability within the system, providing a foundation for future studies, [2], [44].

Extensive research has been conducted on the origins of attraction associated with subharmonic resonance. The authors in, [45] and [46] conducted a study to examine the impact of different parameters, including the amplitude and frequency of the subharmonic component, on the basins of attraction. The investigation of transitions between diverse subharmonic resonant states and the impact of control tactics on the stability boundaries has been examined in previous studies, [47], [48]. Therefore, it is imperative to do additional research on the basins of attraction in order to examine the stability in the event of parameter changes, [49], [50].

2.2 Numerical Analysis
Graphical Representation

The equations (1), (2), and (3) were solved using the fourth-order Runge-Kutta technique in Matlab. The main objective was to investigate the impact of altering the excitation frequency Ω on the phenomenon of subharmonic resonance, [2].

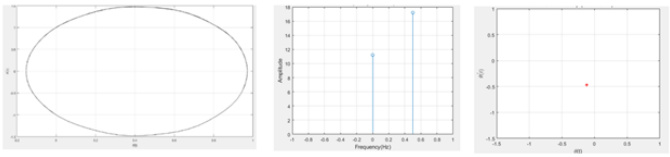

Fig. 2: Phase portrait, frequency-domain plot and Poincaré map when $\Omega = 26.01$ rad/sec, [2].

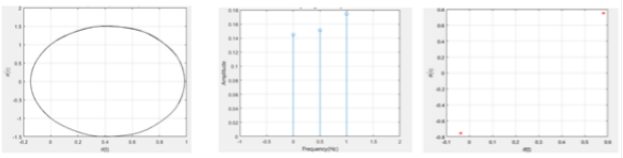

Fig. 3: Phase portrait, frequency-domain plot and Poincaré map when $\Omega = 21.04$ rad/sec, [2].

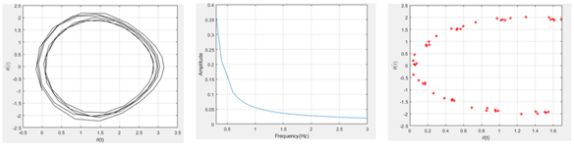

Fig. 4: Phase portrait, frequency-domain plot and Poincaré map when $\Omega = 19.37$ rad/sec, [2].

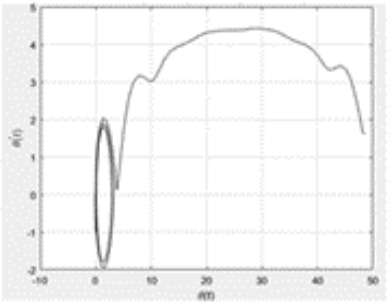

Fig. 5: Phase portrait (loss of synchronism) when $\Omega = 19.37251$ rad/sec, [2].

The phase portraits, frequency-domain plots, and Poincaré maps were generated for the swing equation (1) to yield Figure 2, Figure 3, Figure 4, and Figure 5, which depict the variations in excitation frequency reflected also in, [2]. As the system experiences a reduction, its stability diminishes and it undergoes a cascading process towards a state of chaos. Each plot depicts the many occurrences of period doubling and the subsequent loss of synchrony within the system.

Moreover, as depicted in Figure 3, the period-one orbit undergoes deformation until the angular frequency Ω attains a value of 21.04 rad/sec. At this critical threshold, the period-one attractor ceases to be stable and is subsequently replaced by a period-two attractor. The frequency-domain plot and Poincaré map illustrate the appearance of the period doubling bifurcation, [2].

As the parameter Ω is systematically reduced, it becomes evident that the graphs undergo dynamic changes, such as the emergence of period-doubling solutions. Eventually, as Ω approaches a value of around 19.37 rad/sec, a chaotic attractor is detected, as depicted in Figure 4. The system then experiences a loss of synchronism, as depicted in Figure 5, when the angular velocity (Ω) is reduced to 19.37251 rad/sec, [2].

Figure 6 illustrates the bifurcation diagram and the associated Lyapunov exponents for the instances of primary and subharmonic resonances as echoed in, [2], respectively. The construction process involved calculating the swing equation for a particular angular frequency value of $\Omega = 8.27$ rad/sec for the primary resonance and $\Omega = 19.416$ rad/sec for the subharmonic resonance, followed by numerical time integration using the well-known fourth order Runge-Kutta method. The value of the forcing parameter, denoted as r, is incrementally increased, and the time integration process is continued. The resulting data is then used to create a plot that shows the maximum amplitude of the oscillatory solution as a function of r, [1].

$$r = \frac{V_G V_B}{X_G} sin(\theta - \theta_B)$$

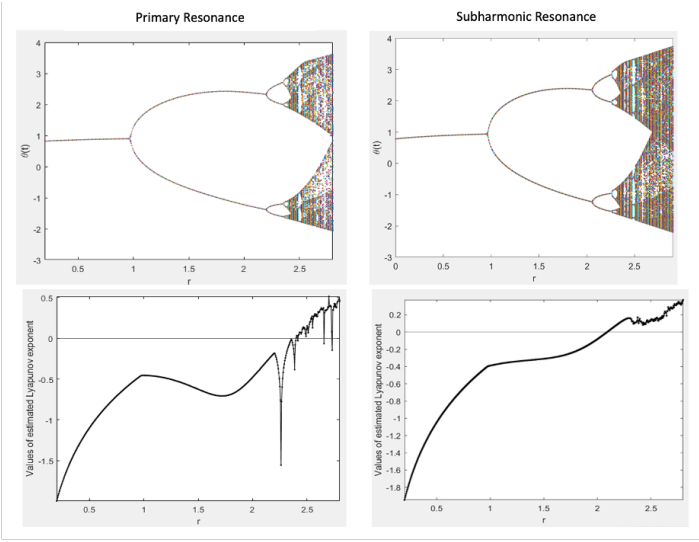

Fig. 6: Bifurcation diagrams and Lyapunov Exponents for Primary and Subharmonic Resonances, [1], [2].

The provided figure, Figure 6, illustrates the occurrence of the initial period doubling just prior to reaching a value of r equal to 0.9 in the case of primary resonance. Additionally, it can be observed that at about r = 2.36, the first instance of period doubling in a series of subsequent period doublings is displayed, ultimately resulting in the emergence of chaotic behaviour. The findings of this numerical analysis indicate that an increase in the value of parameter r leads to a progressive loss of synchronisation in the swing equation, [1].

The phenomenon of subharmonic resonance is characterised by the emergence of a chaotic zone when the value of r exceeds around 2.1, [2]. In this region, the Lyapunov exponent tends to exhibit positive values. The behaviour under consideration is illustrated. In this scenario, two points in close proximity, initially separated by

an infinitesimally small distance, tend to move apart from each other over a period of time. This divergence is quantitatively assessed using the Lyapunov exponents. The behaviour shown in bifurcation diagram further confirms the aforementioned phenomenon. Specifically, once the value of r approaches a certain threshold, a series of period doubling occurs, eventually leading to chaotic behaviour. Consequently, it can be concluded that the presence of a positive Lyapunov exponent is indicative of the existence of a chaotic attractor.

In order to assess the soundness of the analytical solution, a comparison is made between the analytical solution and the numerical simulation. Additionally, a frequency domain plot for equation (39) is depicted in Figure 7, [2]. The findings demonstrate a significant correlation between the two analyses conducted on the swing equation pertaining to subharmonic resonance. Therefore, this paper's analysis is being validated.

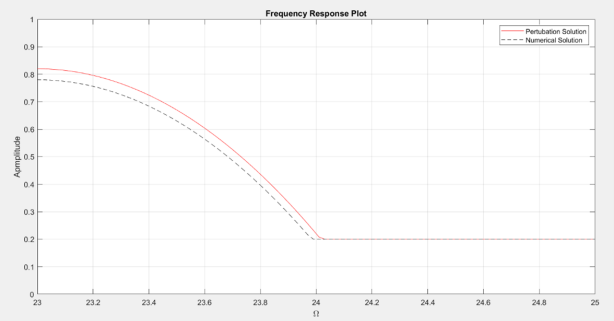

Fig. 7: Frequency domain plot for Subharmonic Resonance, [2].

Figure 8 below compares the numerical results with the analytical methods such as Floquet method, Method of strained parameters and Tangent instability. The application of the Floquet method in MATLAB allows for a comprehensive examination of the stability and dynamic characteristics of the swing equation, hence providing significant insights into the transient stability of power systems. This technique predicts the saddle node bifurcation as shown in the figure but with 9.21% error compared to the numerical result. Method of strained parameters and tangent instability were also solved with computing the solutions for the equation (59) and equation (64) respectively. Method of strained parameters predicts the period-doubling bifurcation with an error of 10.32% when compared to the numerical analysis. Finally the tangent instability method also predicts the saddle node bifurcation with an error of 12.5% compared to its numerical counterpart.

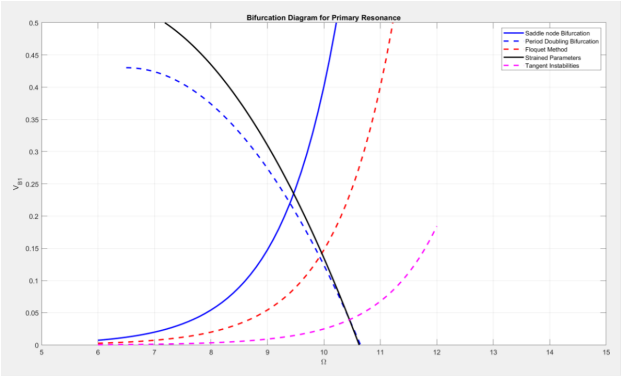

Fig. 8: Bifurcation diagram showing a comparison of different analytical methods for Primary Resonance.

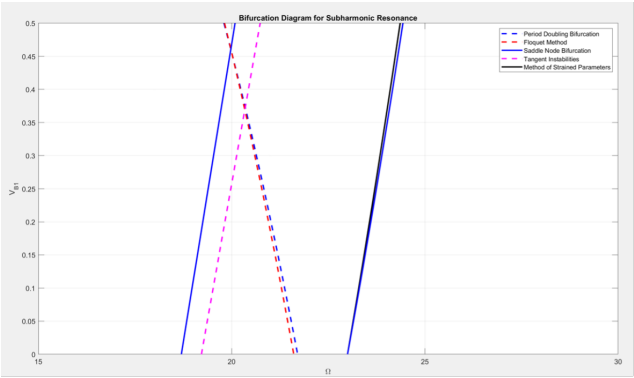

Fig. 9: Bifurcation diagram showing a comparison of different analytical methods for Subharmonic Resonance.

Similarly, Figure 9 presents the contrast between the numerical simulation and the analytical methodologies that have been examined for the case of subharmonic resonance. The time considered is twice that of the primary resonance in this analysis. The Method of Strained Parameters and Tangent Instability have been utilised to forecast saddle node bifurcations, yielding errors of 0.091% and 5.43% respectively, whilst the Floquet method predicts the period doubling bifurcation with 0.102% error compared to the numerical analysis. Some of these predicted methods provide coherency with specific results from, [13].

(i) Basins of attractions for Primary Resonance

The following figures, namely Figure 10, Figure 11, and Figure 12, depict the basins of attraction pertaining to the primary resonance. These

figures illustrate the variations in the variables V_{B1} and θ_{B1} while maintaining a constant value of Ω at 8.27 rad/sec. The stability of the system is subject to change as the variable is raised. The stable portion of the system is shown by the presence of red and green colours, while the remaining colours reflect the unstable regions. As the independent variable is incremented, the system undergoes a state of corruption characterised by the presence of unstable regions. Consequently, it is imperative to conduct a more comprehensive examination of the impact of other variables within the system in order to obtain reliable and robust findings in this particular study.

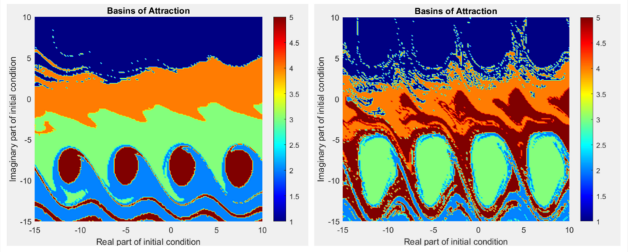

Fig. 10: Basins of attractions when V_{B1} is 0.071 rad and 0.151 rad respectively, [2].

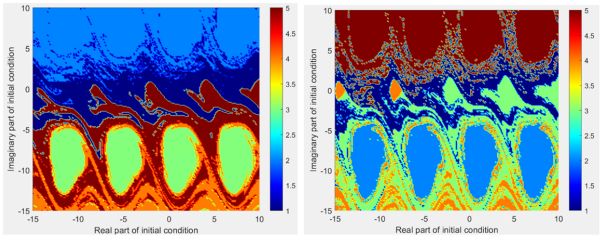

Fig. 11: Basins of attractions when θ_{B1} is 0.191 rad and 0.181 rad respectively.

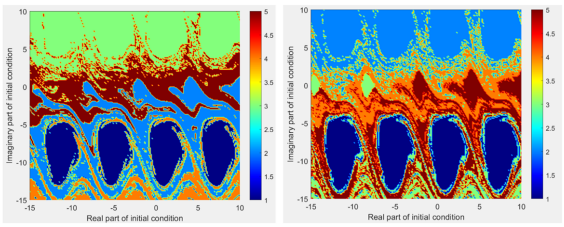

Fig. 12: Basins of attractions when θ_{B1} is 0.141 rad and 0.181 rad respectively.

(ii) Basins of attractions for Subharmonic Resonance

Figure 13 and Figure 14 depict the basins of attraction pertaining to the subharmonic resonance phenomenon in the swing equation of the dynamical system. The variations in V_{B1} and θ_{B1} are considered, while keeping Ω constant at a value of 19.375 rad/sec. According the authors, [2], [13], the corruption of the system occurs as the variable is manipulated. It is vital to study these changes in order to gain a deep understanding of the stability of the system.

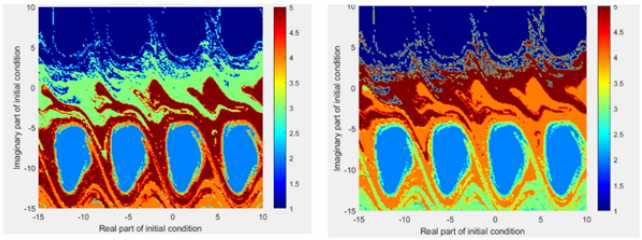

Fig. 13: Basins of attractions when V_{B1} is 0 rad and 0.051 rad respectively, [2].

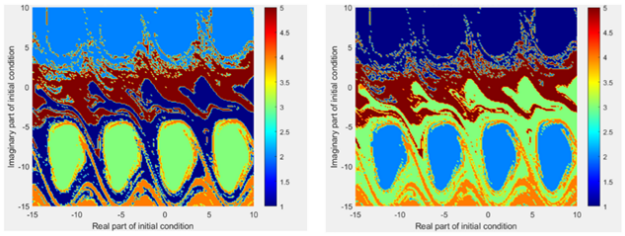

Fig. 14: Basins of attractions when θ_{B1} is 0.191 rad and 0.181 rad respectively, [2].

3 Discussion

The objective of this study is to analyse the dynamic characteristics of the swing equation under different variations of control parameters. This study compares analytical methods, particularly perturbation techniques, with numerical simulation in order to verify the accuracy of the perturbed solution for subharmonic resonance and the basins of attraction associated with these phenomena.

The examination of the primary and subharmonic resonances of the swing equation involves the utilisation of many analytical methods, namely the Floquet method, method of strained parameters, and analytical techniques. These approaches give unique perspectives and contribute

significant knowledge to the understanding of this paper's power system stability. The analytical approach generally depends on the utilisation of mathematical modelling and manual computations, resulting in accurate outcomes within the context of simplified assumptions. However, it may encounter difficulties in accurately representing the many interconnections and non-linear dynamics that manifest in power systems found in real-world scenarios. On the other hand, the Floquet method and the method of strained parameters utilise numerical and computational techniques to effectively address complex dynamics. These methodologies provide a methodical investigation of the system's reaction to diverse conditions and external disturbances, which can be effectively depicted through graphical illustrations. Researchers can enhance their comprehension of the system's behaviour in the vicinity of the primary resonance by graphing the response of the swing equation across various parameter values or forcing frequencies. Graphical analyses serve as a vital supplement to analytical techniques, providing a more holistic perspective on the stability attributes. This aids power system engineers in making well-informed judgements to guarantee the dependable functioning of the grid.

The anticipated response of the system is determined by employing the swing equation in diverse scenarios, including instances involving load alterations. The data is utilised by power system management in order to guarantee the stability and reliability of the system. The use of this approach extends to the design and analysis of control systems for power systems, namely in the areas of autonomous generation control and load frequency management. For instance in the case to mitigate the occurrence of blackouts and the consequential catastrophic consequences they may entail.

4 Conclusion

To summarise, the present study employed various analytical techniques, including bifurcation diagrams, Lyapunov exponents, phase portraits, frequency domain plots, and Poincaré maps, to investigate the dynamics of the swing equation in the context of subharmonic resonance. The occurrence of period doubling in a sequence suggests an impending state of turbulence, which presents potential threats to power systems and operational difficulties. According to research, chaos can be induced by the collapse of quasi-periodic torus structures and the presence of intermittency. Period doubling is a widely recognised illustration.

This study focused on investigating the impact of parameter modifications on the dynamics of the system, specifically highlighting the observed changes before and after the onset of chaotic behaviour. It also highlights and incorporates different methods used to study the stability of the system, such as the Floquet method, Method of strained parameters and Tangent instability. The identification of pre-chaotic motion patterns serves to elucidate the transitory dynamics of a system prior to its entry into a state of chaos. Furthermore, an examination of the basins of attraction pertaining to primary and subharmonic resonances has substantiated the inherent instability of the system, resulting in the manifestation of chaotic phenomena when subjected to subharmonic resonance circumstances.

This study makes a valuable contribution to the current scholarly understanding of the swing equation, namely by offering an extension to the most recent literature authored by the same individuals as this paper, [1], [2]. This research enhances the understanding of the fundamental principles and system stability of the swing equation through a specific emphasis on primary and subharmonic resonances. The discoveries assist power system engineers and researchers in developing improved control strategies and preventive measures to address the chaotic effects caused by subharmonic resonance.

The present study illuminates the dynamic behaviour of the swing equation and its reaction to subharmonic resonance, thereby shedding light on several elements of system stability. This study has the potential to contribute to the development of more resilient and secure power infrastructures, particularly as power systems continue to expand and encounter increasingly complex challenges.

In further research, the incorporation of quasi periodic conditions within the swing equation framework hold the potential to advance the knowledge of this intricate power system. The aforementioned approach has the potential to offer significant insights on the enduring stability and adaptability of the system.

References:

[1] Sofroniou, A., Premnath, B., Munisami, K.J., 2023. An Insight into the Dynamical Behaviour of the Swing Equation 22. https://doi.org/10.37394/23206.2023.22.9

[2] Anastasia Sofroniou, Bhairavi Premnath, "An Investigation into the Primary and Subharmonic Resonances of the Swing Equa-

tion," WSEAS Transactions on Systems and Control, vol. 18, pp. 218-230, 2023. https://doi.org/10.37394/23203.2023.18.22

[3] Ji, J. C., and N. Zhang. "Suppression of the primary resonance vibrations of a forced nonlinear system using a dynamic vibration absorber." Journal of Sound and Vibration 329, no. 11 (2010): 2044-2056.

[4] Nayfeh, A.H. and Mook, D.T., 2008. Nonlinear oscillations. John Wiley Sons

[5] Scholl, T.H., Gröll, L. and Hagenmeyer, V., 2019. Time delay in the swing equation: A variety of bifurcations. Chaos: An Interdisciplinary Journal of Nonlinear Science, 29(12).

[6] Xize, N. and Jiajun, Q., 2002. Investigation of torsional instability, bifurcation, and chaos of a generator set. IEEE Transactions on Energy Conversion, 17(2), pp.164-168.

[7] Sourani, P., Hashemian, M., Pirmoradian, M. and Toghraie, D., 2020. A comparison of the Bolotin and incremental harmonic balance methods in the dynamic stability analysis of an Euler–Bernoulli nanobeam based on the nonlocal strain gradient theory and surface effects. Mechanics of Materials, 145, p.103403.

[8] Liu, C.W. and Thorp, J.S., 1997. A novel method to compute the closest unstable equilibrium point for transient stability region estimate in power systems. IEEE Transactions on Circuits and Systems I: Fundamental Theory and Applications, 44(7), pp.630-635.

[9] Hang, L., Yongjun, S., Xianghong, L., Yanjun, H. and Mengfei, P., 2020. Primary and subharmonic simultaneous resonance of Duffing oscillator. , 52(2), pp.514-521.

[10] Niu, Jiangchuan, Lin Wang, Yongjun Shen, and Wanjie Zhang. "Vibration control of primary and subharmonic simultaneous resonance of nonlinear system with fractional-order Bingham model." International Journal of Non-Linear Mechanics 141 (2022): 103947.

[11] Basler, M.J. and Schaefer, R.C., 2005, April. Understanding power system stability. In 58th Annual Conference for Protective Relay Engineers, 2005. (pp. 46-67). IEEE.

[12] Wang, Xiaodong, Yushu Chen, Gang Han, and Caiqin Song. "Nonlinear dynamic analysis of a single-machine infinite-bus power system." Applied Mathematical Modelling 39, no. 10-11 (2015): 2951-2961.

[13] Nayfeh, Mahir Ali. "Nonlinear dynamics in power systems." PhD diss., Virginia Tech, 1990.

[14] Caliskan, S.Y. and Tabuada, P., 2015, December. Uses and abuses of the swing equation model. In 2015 54th IEEE Conference on Decision and Control (CDC) (pp. 6662-6667). IEEE.

[15] El-Abiad, Ahmed H., and K. Nagappan. "Transient stability regions of multimachine power systems." IEEE Transactions on Power Apparatus and Systems 2 (1966): 169-179.

[16] Sauer, P. W., and M. A. Pai. "Power system steady-state stability and the load-flow Jacobian." IEEE Transactions on power systems 5, no. 4 (1990): 1374-1383.

[17] Qiu, Qi, Rui Ma, Jurgen Kurths, and Meng Zhan. "Swing equation in power systems: Approximate analytical solution and bifurcation curve estimate." Chaos: An Interdisciplinary Journal of Nonlinear Science 30, no. 1 (2020): 013110.

[18] Beltran, O., Peña, R., Segundo, J., Esparza, A., Muljadi, E. and Wenzhong, D., 2018. Inertia estimation of wind power plants based on the swing equation and phasor measurement units. Applied Sciences, 8(12), p.2413.

[19] Emam, Samir A., and Ali H. Nayfeh. "On the nonlinear dynamics of a buckled beam subjected to a primary-resonance excitation." Nonlinear Dynamics 35 (2004): 1-17.

[20] Lin, J.C., 2002. Review of research on low-profile vortex generators to control boundary-layer separation. Progress in aerospace sciences, 38(4-5), pp.389-420.

[21] Arafat, H. N., and A. H. Nayfeh. "Non-linear responses of suspended cables to primary resonance excitations." Journal of Sound and Vibration 266, no. 2 (2003): 325-354.

[22] Zhao, Chongwen, Zhibo Wang, Jin Du, Jiande Wu, Sheng Zong, and Xiangning He. "Active resonance wireless power transfer system using phase shift control strategy." In 2014 IEEE Applied Power Electronics Conference and Exposition-APEC 2014, pp. 1336-1341. IEEE, 2014.

[23] Kavasseri, Rajesh G. "Analysis of subharmonic oscillations in a ferroresonant circuit." International Journal of Electrical Power and Energy Systems 28, no. 3 (2006): 207-214.

[24] Yang, J.H., Sanjuán, M.A. and Liu, H.G., 2016. Vibrational subharmonic and superharmonic resonances. Communications in Nonlinear Science and Numerical Simulation, 30(1-3), pp.362-372.

[25] KISHIMA, Akira. "Sub-harmonic Oscillations in Three-phase Circuit." Memoirs of the Faculty of Engineering, Kyoto University 30, no. 1 (1968): 26-44.

[26] Yang, J.H., Sanjuán, M.A. and Liu, H.G., 2016. Vibrational subharmonic and superharmonic resonances. Communications in Nonlinear Science and Numerical Simulation, 30(1-3), pp.362-372.

[27] Deane, Jonathan HB, and David C. Hamill. "Instability, subharmonics and chaos in power electronic systems." In 20th Annual IEEE Power Electronics Specialists Conference, pp. 34-42. IEEE, 1989.

[28] Nayfeh, M. A., A. M. A. Hamdan, and A. H. Nayfeh. "Chaos and instability in a power system—Primary resonant case." Nonlinear Dynamics 1 (1990): 313-339.

[29] Wang, Dong, Junbo Zhang, Wei Cao, Jian Li, and Yu Zheng. "When will you arrive? estimating travel time based on deep neural networks." In Proceedings of the AAAI Conference on Artificial Intelligence, vol. 32, no. 1. 2018.

[30] Zhang, Wei, Fengxia Wang, and Minghui Yao. "Global bifurcations and chaotic dynamics in nonlinear nonplanar oscillations of a parametrically excited cantilever beam." Nonlinear Dynamics 40 (2005): 251-279.

[31] Haque, M.T. and Kashtiban, A.M., 2007. Application of neural networks in power systems; a review. International Journal of Energy and Power Engineering, 1(6), pp.897-901.

[32] Klausmeier, C.A., 2008. Floquet theory: a useful tool for understanding nonequilibrium dynamics. Theoretical Ecology, 1, pp.153-161.

[33] Païdoussis, M.P. and Semler, C., 1993. Nonlinear and chaotic oscillations of a constrained cantilevered pipe conveying fluid: a full nonlinear analysis. Nonlinear Dynamics, 4, pp.655-670.

[34] Eldabe, N.T., 1989. Effect of a tangential electric field on Rayleigh-Taylor instability. Journal of the physical society of Japan, 58(1), pp.115-120.

[35] Eldabe, N.T., 1989. Effect of a tangential electric field on Rayleigh-Taylor instability. Journal of the physical society of Japan, 58(1), pp.115-120.

[36] Kuznetsov, Yuri A., Iu A. Kuznetsov, and Y. Kuznetsov. Elements of applied bifurcation theory. Vol. 112. New York: Springer, 1998.

[37] Alsaleem, F.M., Younis, M.I. and Ouakad, H.M., 2009. On the nonlinear resonances and dynamic pull-in of electrostatically actuated resonators. Journal of Micromechanics and Microengineering, 19(4), p.045013.

[38] Haberman, R. and Ho, E.K., 1995. Boundary of the basin of attraction for weakly damped primary resonance.

[39] Van Cutsem, Thierry, and C. D. Vournas. "Emergency voltage stability controls: An overview." In 2007 IEEE Power Engineering Society General Meeting, pp. 1-10. IEEE, 2007.

[40] Yılmaz, Serpil, and Ferit Acar Savacı. "Basin stability of single machine infinite bus power systems with Levy type load fluctuations." In 2017 10th International Conference on Electrical and Electronics Engineering (ELECO), pp. 125-129. IEEE, 2017.

[41] Najar, F., Nayfeh, A.H., Abdel-Rahman, E.M., Choura, S. and El-Borgi, S., 2010. Dynamics and global stability of beam-based electrostatic microactuators. Journal of Vibration and Control, 16(5), pp.721-748.

[42] Parashar, Manu, James S. Thorp, and Charles E. Seyler. "Continuum modeling of electromechanical dynamics in large-scale power systems." IEEE Transactions on Circuits and Systems I: Regular Papers 51, no. 9 (2004): 1848-1858.

[43] Soliman, M.S., 1995. Fractal erosion of basins of attraction in coupled non-linear systems. Journal of sound and vibration, 182(5), pp.729-740.

[44] Nayfeh, M.A., Hamdan, A.M.A. and Nayfeh, A.H., 1991. Chaos and instability in a power system: subharmonic-resonant case. Nonlinear Dynamics, 2, pp.53-72.

[45] Pecora, Louis M., Thomas L. Carroll, Gregg A. Johnson, Douglas J. Mar, and James F. Heagy. "Fundamentals of synchronization in chaotic systems, concepts, and applications."

Chaos: An Interdisciplinary Journal of Nonlinear Science 7, no. 4 (1997): 520-543.

[46] Dixit, Shiva, and Manish Dev Shrimali. "Static and dynamic attractive–repulsive interactions in two coupled nonlinear oscillators." Chaos: An Interdisciplinary Journal of Nonlinear Science 30, no. 3 (2020).

[47] Al-Qaisia, A. A., and M. N. Hamdan. "Subharmonic resonance and transition to chaos of nonlinear oscillators with a combined softening and hardening nonlinearities." Journal of sound and vibration 305, no. 4-5 (2007): 772-782.

[48] Butikov, Eugene I. "Subharmonic resonances of the parametrically driven pendulum." Journal of Physics A: Mathematical and General 35, no. 30 (2002): 6209.

[49] Nusse, Helena E., and James A. Yorke. Dynamics: numerical explorations: accompanying computer program dynamics. Vol. 101. Springer, 2012.

[50] Wuensche, A., 2004. Basins of attraction in network dynamics. Modularity in development and evolution, pp.1-17.

Contribution of individual authors to the creation of a scientific article (ghostwriting policy)

All authors contributed to the development of this paper. Conceptualisation, Anastasia Sofroniou; Methodology, Anastasia Sofroniou and Bhairavi Premnath; Analytical and Numerical Analysis Bhairavi Premnath; Validation, Anastasia Sofroniou and Bhairavi Premnath; Writing-original draft preparation, Bhairavi Premnath and Anastasia Sofroniou; Writing-review and editing, Anastasia Sofroniou and Bhairavi Premnath; Supervisor, Anastasia Sofroniou.

Sources of Funding for Research Presented in a Scientific Article or Scientific Article Itself

No funding was received for conducting this study.

Conflict of Interest

The authors have no conflicts of interest to declare that are relevant to the content of this article.